

# Aortic Root Dynamics are Asymmetric

Emmanuel Lansac<sup>1</sup>, Hou-Sen Lim, Yu Shomura, Khee Hiang Lim, Nolan T. Rice, Wolfgang A. Goetz, Carlos M. G. Duran

*The International Heart Institute of Montana Foundation at St. Patrick Hospital and Health Sciences Center and The University of Montana, Missoula, Montana, USA*

<sup>1</sup>*Present address: Chirurgie Thorecique et Cardiovasculaire, Hospital Pitie-Salpetriere, Paris, France*

**Background and aim of the study:** The presence of conformational changes in the aortic root during the cardiac cycle is well known, but precise information on time-related changes at each level of the root is lacking.

**Methods:** High-resolution, 3D sonomicrometry (200 Hz) was applied in an acute sheep model. Twelve crystals were implanted in eight sheep at each base (n = 3), commissure (n = 3), sinotubular junction (n = 3) and ascending aorta (n = 3). Under stable hemodynamic conditions, geometric changes of the perimeter of each sinus of Valsalva, sinus height, and twist and root tilt angles were time-related to left ventricular (LV) and aortic pressures.

**Results:** Expansion of the perimeter of the three sinuses of Valsalva was homogeneous, but in significantly different proportions (p <0.001): the right sinus expanded (+32.4 ± 2.4%) more than the left (+29.3 ± 3.2%), and more than the non-coronary (NC) sinus (+25.8 ± 1.7%). A similar pattern was found for

aortic root height: right greater than left, and left greater than NC sinus (p <0.001). This asymmetry resulted in changes of the root's twist and tilt angles. Although the twist deformation was consistent for each sheep, no general pattern was found. The aortic root tilt angle (between the basal plane and the commissural plane) was 16.3 ± 1.5° at end-diastole (angle oriented posteriorly and to the left). During systole, it was reduced by 6.6 ± 0.5°, aligning the LV outflow tract with the ascending aorta. This tilt angle returned to its original value after valve closure.

**Conclusion:** Aortic root expansion is asymmetric, generating precise changes in its tilt angle. During systole, tilt angle reduction resulted in a straight cylinder that probably facilitates ejection; during diastole, the tilt angle increased, probably reducing leaflet stress. These findings should impact upon surgical procedures and the design of new prostheses.

The Journal of Heart Valve Disease 2005;14:400-407

The increased popularity of stentless valves (1-3), aortic valve reconstruction with pericardium (4,5) and valve-sparing procedures (6-8) demands a better understanding of the anatomy and physiology of the aortic valve complex. The importance of the sinuses of Valsalva for the opening and closure of the aortic valve was intuitively shown by Leonardo da Vinci (9) and confirmed 500 years later by Bellhouse and Bellhouse (10) in an in-vitro model. Early in-vivo dynamic studies of the aortic root showed its significant expansion

during the cardiac cycle, but without consideration of the possible asymmetry of each sinus (11-13). Becker's group (14) showed the complete asymmetry between sinuses in a large post-mortem study of human aortic roots, whilst more recently Choo et al. (15) showed the presence of a particular pattern in this symmetry. Recent dynamic studies with better instrumentation have shown in vivo that this anatomic asymmetry corresponds to a dynamic deformation of the aortic root (16,17). However, information on the precise time-related geometric changes of the individual components of the root during the cardiac cycle is lacking. The present study considered that the normal aortic root is basically formed by three unequal sinuses of Valsalva (15) that, by behaving differently during the cardiac cycle, determine significant conformational changes of the whole root that might have hemodynamic consequences. The use of three-dimensional (3D) sonomicrometry, which provides 200 data points

---

Presented at the First Biennial Meeting of the Society for Heart Valve Disease, 15th-18th June 2001, Queen Elizabeth II Conference Centre, London, United Kingdom

Address for correspondence:  
Carlos M. G. Duran MD, DPhil, The International Heart Institute of Montana, 554 West Broadway, Missoula, Montana 59802, USA  
e-mail: duran@saintpatrick.org

per second, has further elucidated this issue (18-20). Herein are reported the findings with this technique in an acute, open-chest sheep model.

## Materials and methods

### Animals

Eight adult sheep (mean  $\pm$  SEM body weight  $42.5 \pm 2$  kg) underwent implantation of 12 ultrasonic crystals in the aortic root using cardiopulmonary bypass (mean pump time  $158 \pm 8$  min; mean cross-clamp time  $74 \pm 3$  min). All animals received humane care in compliance with the principles of the Animal Welfare Act, the *Guide for Care and Use of Laboratory Animals* from the United States Department of Agriculture, and approved by The Institutional Animal Care and Use Committee of The University of Montana.

### Surgical protocol

Anesthesia was induced with intravenous ketamine (1.0 mg/kg) and propofol (4.0 mg/kg) and maintained with endotracheal isoflurane (1.5-2.5%). The electrocardiogram (ECG) was monitored continuously. Artificial ventilation was achieved with a volume-regulated respirator (North American Drager, Telford, PA, USA) supplemented with oxygen at 2 l/min. The heart was exposed with a standard left thoracotomy through the fourth intercostal space. The left femoral (16 Fr) and left internal thoracic (10 Fr) arteries were cannulated. A venous cannula was inserted into the right atrium (32 Fr). The aorta and single arch vessel were cross-clamped, and cold, crystalloid cardioplegia was infused into the root. Twelve ultrasonic crystals (Sonometrics Corporation, London, Ontario, Canada) were implanted through a transverse aortotomy approximately 1 cm distal to the sinotubular junction (STJ) to study the aortic valve complex. To avoid inter-operator variability, the same surgeon placed all crystals. Ultrasonic crystals (1 mm) were placed and secured with 5-0 polypropylene sutures at: (i) the lowest point of each sinus of Valsalva, corresponding to the so-called aortic base (B;  $n = 3$ ); (ii) the aortic commissures (C;  $n = 3$ ); (iii) the highest point of each supra-aortic crest or STJ ( $n = 3$ ); and (iv) at the wall of the ascending aorta (AA;  $n = 3$ ) (Fig. 1). On the ascending aorta, the left, right and non-coronary (NC) crystals were lined up with the crystals placed at the left, right and NC of the base and STJ. The crystals were oriented so that they all pointed toward the lumen. The crystal's electrodes were exteriorized through the aortic wall at each point of insertion to reduce their possible interference with aortic valve movements. High-fidelity, catheter-tipped pressure transducers (Model 510; Millar Instruments, Houston, TX, USA) were placed in the proximal ascending aorta and in the left ventricu-

lar (LV) cavity. A flowmeter ring was placed around the ascending aorta (Transonic flowmeter T206; Transonic Systems, Ithaca, NY, USA).

### Experimental design

After discontinuing cardiopulmonary bypass and when the animal was hemodynamically stable (at least 15 min), recordings were taken at 200 Hz. Epicardial two-dimensional (2D) color Doppler echocardiography was used to confirm the competence of the aortic valve. At the end of the experiment, the heart was arrested by lethal injection of potassium chloride, explanted, and the correct position of the crystals was checked.

### Definition of different phases of the cardiac cycle

The aortic root geometric changes were time-related to each phase of the cardiac cycle, as defined from the aortic and LV pressure tracings (Fig. 2) (21,22). End-diastole, or beginning of systole (beginning of isovolumic contraction), was defined as the beginning of LV pressure increase ( $dP/dt > 0$ ). The end of isovolumic contraction, or beginning of ejection, was determined at the crossing point of the LV and aortic pressure tracings (gradient aortic/LV pressure = 0). The dicrotic notch in the aortic pressure curve defined end ejection. The end of isovolumic relaxation was defined as the lowest point of LV pressure after ejection ( $dP/dt = 0$ ) (17).

### Definition of aortic root anatomic regions

The aortic root and the ascending aorta were each divided into four cross-sectional areas defined by three crystals: basal, commissural, STJ, and ascending aorta (Fig. 1). The perimeter of the sinuses of Valsalva (right, left, NC) was defined by one area calculated from four

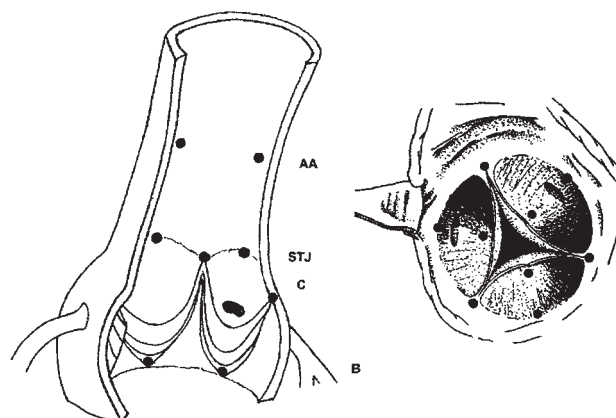


Figure 1: Location of the sonomicrometry crystals (black dots) in the aortic root. AA: Ascending aorta; B: Base; C: Commissures; STJ: Sinotubular junction.

crystals (basal, STJ, and two adjacent commissures) and two lengths (intercommissural distance and root height). Left, right and NC intercommissural lengths were defined as the distances between each pair of commissural crystals. The root height was defined by the distance between crystals at the STJ and the base of each sinus of Valsalva. The right-left, left-NC and NC-right coronary sinus basal lengths were defined as the distances between each pair of basal crystals.

**Data acquisition and calculation of aortic root deformation**

Sonometrics Digital Ultrasonic Measurement System TRX Series 1-mm transmitter/receiver crystals were used to measure displacements. A post-processing program (Sonometrics Corporation) was used to examine each individual length between crystals and for 3D reconstruction of the crystal coordinates. All distances, pressures and flows were synchronized and recorded at the same time line on the same screen using the

Sonometrics system.

Length data were obtained directly from the measured distances between pairs of crystals, and Lagrangian strain was used to define the deformation from the original length at end-diastole (23). Each level of the aortic root was represented by a triangular area defined from the three corresponding crystals and calculated using Heron's formula (24). A post-processing program (Sonovol; Sonometrics Corporation) was used to calculate aortic root volumes using the convex hull approach. Crystals at the base, commissures and STJ were used for these calculations. Methods to calculate these parameters are provided in Appendix I.

The angle between the plane formed by the three basal crystals and the plane formed by the three commissural crystals was calculated using Vector and Analytic Geometry in Space (25). This angle was identified as the aortic root tilt angle. For each sinus, a shear angle was calculated using two adjacent commissural crystals and the corresponding basal crystal

*Table I: Changes in the aortic root during the cardiac cycle. Data are displayed: (i) as percent changes of area or lengths relative to total change over the entire cycle; (ii) as raw area value.*

Parameter	IVC	Ejection (first third)	Ejection (last two-thirds)	IVR	Mid-diastole	End-diastole	Total expansion
Right sinus area (%)	+30.9 ± 2.5*	+69.0 ± 2.5*	-50.0 ± 2.4*	-39.1 ± 1.8*	-18.6 ± 2.2*	+7.8 ± 1.1*	32.4 ± 2.4*
Area (mm <sup>2</sup> )	76.3 ± 4.4	91.9 ± 4.4	81.2 ± 3.8	72.6 ± 4.1	68.3 ± 4.1	70.0 ± 4.5	22.0 ± 2.1
Left sinus area (%)	+34.6 ± 3.9*	+65.3 ± 3.9*	-49.8 ± 2.1*	-44.9 ± 2.8*	-16.1 ± 2.0*	+10.9 ± 1.8*	29.3 ± 3.2*
Area (mm <sup>2</sup> )	100.7 ± 6.2	117.7 ± 6.0	105.3 ± 5.5	93.8 ± 7.2	89.4 ± 7.0	92.2 ± 6.9	25.6 ± 3.8
NC sinus area (%)	+24.7 ± 2.4*	+75.2 ± 2.4*	-61.3 ± 4.1*	-29.7 ± 2.5*	-18.4 ± 2.5*	+9.5 ± 2.7*	25.8 ± 1.7*
Area (mm <sup>2</sup> )	69.8 ± 4.8	82.4 ± 3.8	72.8 ± 3.6	67.8 ± 4.8	64.7 ± 4.2	66.0 ± 4.6	16.4 ± 1.4
Right sinus height (%)	+27.5 ± 3.0*	+72.5 ± 3.0*	-12.0 ± 2.5*	-57.1 ± 5.6*	-36.9 ± 3.1*	+5.9 ± 2.0*	11.5 ± 1.0*
Length (mm)	11.3 ± 0.9	12.1 ± 0.9	11.9 ± 0.9	11.3 ± 0.9	10.9 ± 0.9	10.9 ± 0.9	1.2 ± 0.1
Left sinus height (%)	+44.5 ± 6.6*	+53.5 ± 6.4*	-17.5 ± 4.1*	-79.8 ± 11.4*	-22.2 ± 3.7*	+21.5 ± 6.8*	8.7 ± 1.4*
Length (mm)	12.7 ± 0.8	13.2 ± 0.8	13.0 ± 0.8	12.3 ± 0.8	12.1 ± 0.8	12.2 ± 0.8	1.0 ± 0.3
NC sinus height (%)	+43.4 ± 6.3*	+56.3 ± 6.3*	-24.7 ± 4.8*	-66.1 ± 11.4*	-32.0 ± 6.2*	+23.1 ± 11.7*	5.1 ± 0.6*
Length (mm)	10.5 ± 0.5	10.8 ± 0.5	10.6 ± 0.5	10.4 ± 0.4	10.2 ± 0.4	10.2 ± 0.5	0.5 ± 0.1
Right inter-commissural length (%)	+32.8 ± 4.0*	+67.1 ± 4.0*	-64.8 ± 2.0*	-29.4 ± 2.7*	-11.5 ± 1.9*	+5.8 ± 2.0*	26.7 ± 1.5*
Length (mm)	13.0 ± 0.4	15.2 ± 0.6	13.1 ± 0.5	12.1 ± 0.5	11.7 ± 0.4	12.0 ± 0.4	3.3 ± 0.3
Left inter-commissural length (%)	+37.6 ± 3.8*	+62.3 ± 3.7*	-65.6 ± 2.9*	-36.3 ± 2.9*	-8.5 ± 1.7*	+10.4 ± 4.1*	24.4 ± 1.3*
Length (mm)	13.7 ± 0.6	15.5 ± 0.4	13.7 ± 0.5	12.8 ± 0.5	12.5 ± 0.5	12.7 ± 0.5	2.9 ± 0.3
NC inter-commissural length (%)	+35.1 ± 4.9*	+64.8 ± 4.9*	-62.6 ± 1.5*	-32.0 ± 2.4*	-10.5 ± 1.8*	+5.2 ± 1.5*	31.3 ± 2.2*
Length (mm)	12.4 ± 0.7	14.8 ± 0.6	12.6 ± 0.5	11.6 ± 0.6	11.2 ± 0.6	11.3 ± 0.6	3.5 ± 0.3
Right-left basal length (%)	+52.1 ± 5.0*	+47.9 ± 5.0*	-53.5 ± 2.4*	-42.2 ± 2.9*	-14.6 ± 1.3*	+10.4 ± 3.4*	19.2 ± 2.0*
Length (mm)	17.8 ± 0.6	19.4 ± 0.3	17.8 ± 0.5	16.6 ± 0.6	16.2 ± 0.6	16.4 ± 0.6	3.0 ± 0.5
Left-NC basal length (%)	+37.8 ± 8.5*	+44.5 ± 0*	-37.7 ± 7.6*	-40.5 ± 13.1*	-37.5 ± 3.8*	+33.4 ± 5.5*	12.9 ± 2.0*
Length (mm)	17.7 ± 1.3	18.8 ± 1.1	18.1 ± 1.1	16.9 ± 1.1	16.2 ± 1.2	16.8 ± 1.3	2.0 ± 0.5
NC-Right basal length (%)	+49.5 ± 4.6*	+45.7 ± 4.2*	-110.2 ± 18.9*	-10.0 ± 13.5*	-10.6 ± 2.5*	+35.6 ± 6.7*	8.4 ± 0.8*
Length (mm)	19.9 ± 0.8	20.7 ± 0.7	19.3 ± 0.8	18.9 ± 0.9	18.7 ± 0.9	19.2 ± 0.8	1.5 ± 0.2

Results are expressed as mean ± SEM.

\*p < 0.001. A univariate generalized linear model was used to test for significant differences.

IVC: Isovolumic contraction; IVR: Isovolumic relaxation; NC: Non-coronary sinus.

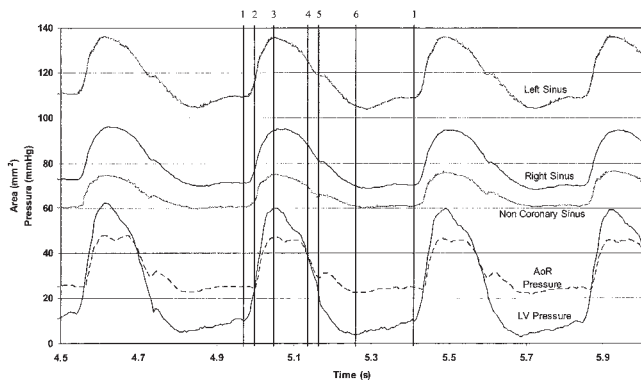


Figure 2: Dynamic changes of the right, left, and non-coronary sinus of Valsalva perimeter area time related to left ventricular (LV) and aortic root pressures. Each curve shows the systolic and diastolic changes in the surface of each sinus of Valsalva. Vertical lines define the beginning of each phase of the cardiac cycle as described in Table I. 1, isovolumic contraction; 2, ejection (first third); 3, ejection (last two-thirds); 4, isovolumic relaxation; 5, mid-diastole; 6, end-diastole.

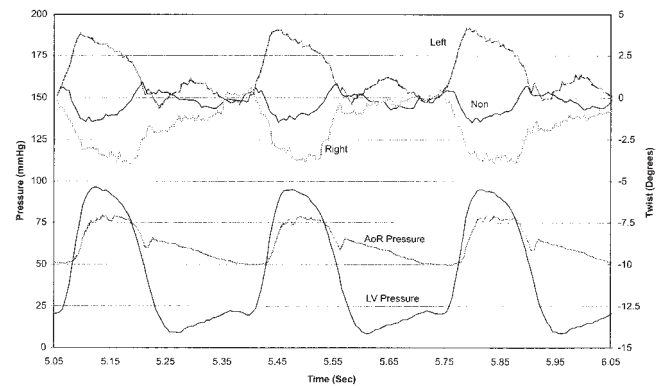


Figure 3: Dynamic changes of the twist angle of the sinuses of Valsalva time related to left ventricular (LV) and aortic root pressures. Note that the left coronary sinus is twisting in opposite direction to the non- and right coronary sinuses during systole (sheep 7). Left: Left coronary sinus; Right: Right coronary sinus; Non: Non-coronary sinus.

with the 2D Green's theorem (25). The twist deformation was calculated from the instantaneous shear angle, root diameter and root height, and was defined as the twist angle between the plane of the base and the plane of the STJ for each sinus of Valsalva (26).

Changes in length, area and volume were defined by: (i) total percentage change with reference to the original value at end-diastole; and (ii) proportional percentage change during each phase of the cardiac cycle relative to the total changes over the entire cycle.

### Statistical analysis

After close examination of the data, the three consecutive heartbeats that contained the least amount of noise were chosen for analysis. The summary statistics were reported as mean  $\pm$  SEM. Univariate generalized linear model (GLM) statistical methods were used to test for significant differences (significance level,  $p < 0.001$ ). All statistical analyses were carried out using the SPSS 0.9 program (SPSS, Inc. Chicago, IL, USA).

## Results

### Experimental conditions

At the time of recording, hemodynamic conditions were: heart rate  $145 \pm 8$  beats/min; aortic pressure  $70/45 \pm 5/4$  mmHg; stroke volume  $20 \pm 2$  ml; and cardiac output  $2.8 \pm 0.3$  l/min. Seven sheep had no regurgitation, and one animal had trivial regurgitation on epicardial echocardiography control. At necropsy, all crystals were confirmed to be in the correct position.

### Asymmetric aortic root expansion

During the cardiac cycle, the aortic root volume increased by  $33.7 \pm 2.7\%$ . Each level of the aortic root underwent a cyclic deformation in three phases: (i) expansion during the isovolumic contraction and the first third of ejection; (ii) a decrease during the last two-thirds of ejection until mid-diastole; and (iii) re-expansion during end-diastole (Fig. 2; Table I).

The expansion of the root was asymmetrical (Table I). During systole, the percentage area expansion of the perimeter of each sinus of Valsalva was significantly

Table II: Changes in tilt angle of the aortic root during the cardiac cycle in relation to its maximum value at end-diastole ( $16.3 \pm 1.5^\circ$ ).

	IVC	Ejection (first third)	Ejection (last two-thirds)	IVR	Mid-diastole	End-diastole	Total change
Tilt angle ( $^\circ$ )	$-2.1 \pm 0.3$	$-4.1 \pm 0.7$	$+1.4 \pm 0.2$	$+2.8 \pm 0.3$	$+2.3 \pm 0.3$	$-0.4 \pm 0.3$	$6.6 \pm 0.5$

Results are expressed as mean  $\pm$  SEM.

IVC: Isovolumic contraction; IVR: Isovolumic relaxation.

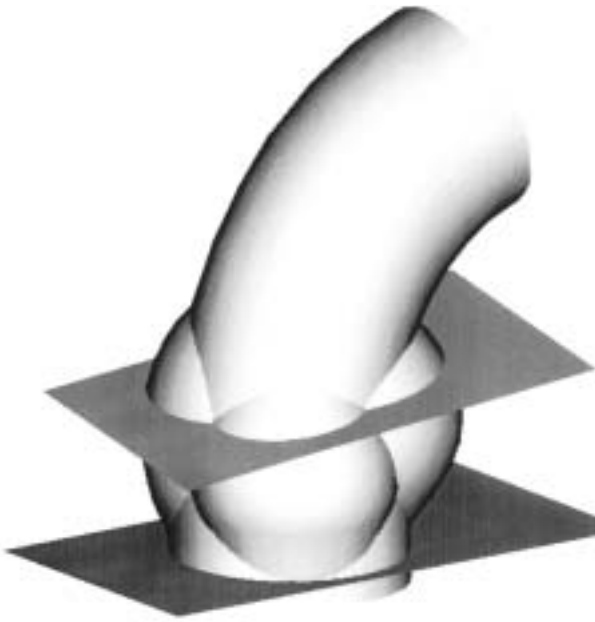


Figure 4: Diagram of the tilt angle between the basal and commissural planes of the aortic root at end-diastole ( $16.3 \pm 1.5^\circ$  and oriented posterior and to the left).

different ( $p < 0.001$ ): the right expanded more than the left, and more than the NC sinus. The same pattern was found for the increase in each sinus height ( $p < 0.001$ ). However, the intercommissural distances followed a different pattern ( $p < 0.001$ ): the NC expanded more than the right and more than the left. All three basal lengths expanded during ejection, but to a different degree ( $p < 0.001$ ). The right to left distance expanded more than the left to NC, and more than the NC to right base. In other words, during systole, the septal portion of the aortic annulus (NC-right basal length) expanded the least, while the aortomitral junction (corresponding to the left-NC basal length) expanded by  $+12.9 \pm 2.0\%$ .

#### Changes in twist and tilt angles during the cardiac cycle

The asymmetrical expansion of the perimeter of the sinuses of Valsalva indicated a rotation or twist of the root and a change in the tilt angle between the basal and the commissural planes. As shown in Figure 3, the left sinus changed first, followed by the non-coronary and then the right, resulting in an anti-clockwise rotation, as seen from the aorta. This deformation was heterogeneous because when one sinus was systematically expanding, the other two were contracting with a delay, resulting in a clockwise or anti-clockwise twist. Although this twist deformation between the three sinuses was consistent within each sheep, no general pattern was found. It was not the same sinus

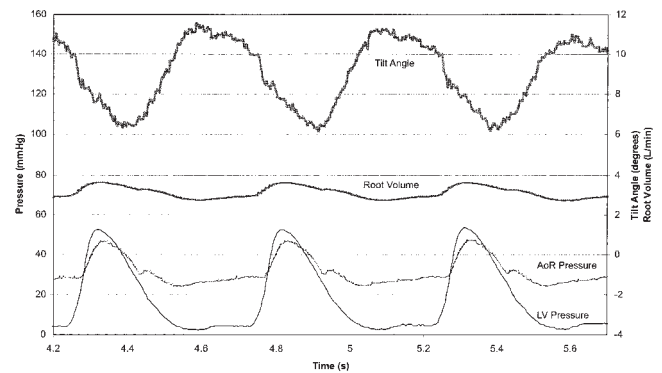


Figure 5: Dynamic changes of tilt angle of the aortic root time related to left ventricular and aortic pressures. AoR: Aortic pressure; LV: Left ventricular pressure.

that always started twisting in the opposite direction to the other two sinuses in every sheep. In four of six sheep, the left coronary sinus was the initiator, in the other two it was the right, and in no case, the non-coronary sinus.

A pattern was found in the aortic tilt angle formed by the basal and commissural planes (Fig. 4). At end-diastole, the aortic root was tilted by  $16.3 \pm 1.5^\circ$  and oriented posteriorly and toward the left. The degree of tilting was inversely related to the root expansion (Fig. 5). During systole, the root tilt angle was reduced by  $6.6 \pm 0.5^\circ$  while the root expanded (Table II). In other words, the root became a straighter cylinder. As soon as the aortic root volume began to decrease and the aortic valve started to close during the second half of ejection, the tilt angle increased toward its initial diastolic value - that is, the root became more curved (Fig. 5). Most of this recoil occurred after aortic valve closure during the isovolumic relaxation until mid-diastole. During end-diastole, although the aortic root volume re-increased by  $11.3 \pm 2.4\%$ , the tilt angle started to decrease before the beginning of a new cycle.

#### Discussion

During the 1970s, Brewer et al. (11), followed by Thubrikar et al. (12,13), pioneered the field of aortic dynamic anatomy. These authors described commissural expansion during the cardiac cycle as part of the initial mechanism of valve opening to reduce shear stress on the leaflets. Most anatomic descriptions have reported an asymmetric aortic root with random variability in the size of different structures of the aortic root (14) or following particular patterns according to species. The pattern of a larger, non-coronary sinus followed by the right and then by the left has been described for the human heart. This difference in sinus size corresponded to their volume, height, width and leaflet size and thickness (15,27-30). In an anatomic

study of the aortic valve in different species, Sands et al. (27) found significant differences between the human and the sheep. Whether this difference in size between sinuses has particular consequences in the dynamics of the aortic root remains to be shown. In the present study, the area of the left coronary sinus perimeter was the largest in all sheep, but the pattern of the left being larger than the right and, in turn, larger than the non-coronary was present in only half of the animals. However, the order of sinus expansion was the right first, followed by the left, and then the non-coronary sinus. The anatomic position of the sinus and the presence of coronary ostia might possibly play an important role in the order of sinus expansion.

In 1988, van Renterghem et al. (16) first described aortic annular base dynamics based on a sampling rate of 150 images per second. This group showed that during ejection, the basal segments adjoining the myocardium (NC-right, and right-left basal lengths) shortened while the aortomitral junction (left-NC basal length) lengthened. The present study with a data acquisition of 200 images per second confirmed van Renterghem's findings. The base and commissural areas changed homogeneously - that is, they all expanded and recoiled similarly during the cardiac cycle. However, significant ( $p < 0.001$ ) differences in the degree of expansion between the individual segments of the root base were observed. The septal portion (NC-right) of the base of the aortic root expanded the least ( $8.4 \pm 0.8\%$ ), whereas the aortomitral junction (corresponding to the NC-left basal length) expanded by  $+12.9 \pm 2.0\%$ .

Dagum et al. (17) described the shear and torsion deformation of the aortic root during the cardiac cycle using six videofluoroscopic (60 Hz) markers in an ovine model. Despite the fact that these studies used triplets of markers defining each interleaflet triangle (one commissural and two basal), and the present data were calculated using triplets of markers defining each sinus of Valsalva (one basal and two commissural), both studies show a heterogeneous torsion of the three sinuses of Valsalva - that is, one sinus twisting in the opposite direction to the other two. The underlying mechanism and physiological relevance of these findings is unknown. It could be hypothesized that the twist deformation of the aortic root is somehow related to the presence of the coronary ostia in only two sinuses (and/or dominance in the coronary circulation) because the non-coronary sinus never twisted in opposition to the other two, and the left coronary sinus was the most involved in this dynamic.

The observed pattern in the changes of the aortic root tilt angle might have more obvious physiological relevance. Previously, an 11-degree angle was described between the plane of the base and the plane of the

sinotubular junction in pressurized and fixed isolated cryopreserved human aortic roots (15). The present study describes the tilting dynamics of the aortic root during the cardiac cycle for the first time. Despite model and species differences, both maximum angles were similar (human  $11^\circ$  versus sheep  $16.3^\circ$ ). The angle changed inversely to the aortic root expansion. During systole - while the root expanded - the tilt angle decreased, whereas during diastole - as the root recoiled - the angle increased. When the angle is reduced during ejection (valve opening), the plane of the base and the plane of the commissures become more parallel, lining up the LV outflow tract with the ascending aorta and therefore maximizing ejection. During diastole, the angle tilts back to its original angle ( $16.3 \pm 1.5^\circ$  oriented posterior and left), mainly after aortic valve closure. This geometric change suggests a possible mechanism as a shock absorber to reduce shear stress on the leaflets while LV pressure is dramatically falling.

The present findings highlight the need to approach the aortic valve as a precise and delicate apparatus that must include the whole aortic root and possibly the coronary arteries, mitral valve and LV outflow tract. A better understanding of this complex mechanism should impact upon the development of new surgical interventions and the design of new prostheses.

### Study limitations

The main limitation of the present study was the invasive, acute and open-chest nature of the animal model. The deleterious effect of cardiopulmonary bypass and ischemia might have resulted in an abnormal aortic root behavior. It could also be argued that the high heart rate present at the time of data acquisition (probably due to catecholamine release) might alter aortic root motion recorded during the shorter cardiac cycles. No autonomic blockade was used to avoid LV function depression. The blood pressure and stroke volume at recording was lower by 10-20 mmHg compared with pre-bypass measurements. Therefore, expansion of the aortic root might have been underestimated compared with normal physiological conditions. It must be specified that the aortic root volume measured using the convex hull approach did not include the entire volume of each sinus, but corresponded to the volume of a cylindrical portion of the aortic root defined by nine crystals (base, commissures, STJ). However, the consistent pattern found in all animals - and the fact that all geometric changes were related to the cardiac phases - advocates the validity of these findings. A possible source of error due to the presence of crystals and attached electrodes is inherent to all marker techniques. The aortic root electrodes were passed through the aortic wall at each

location and were therefore outside the aortic lumen. Furthermore, variability in the precise location of the crystals must be considered, though in an attempt to avoid this problem all operations were performed by the same surgeon. Finally, it must be noted that this study was conducted in young sheep with a very elastic aortic root; in comparative terms, the human adult aortic root may behave differently.

### Acknowledgements

The authors express their sincerest thanks to Kathleen Billington and Leslie Trail for their effort, advice and support that was essential to the completion of these studies. They also thank Reed Mandelko for the illustrations and Jill Roberts for her editorial assistance.

### References

1. Ross DN. Replacement of aortic and mitral valves with a pulmonary autograft. *Lancet* 1967;2:956-958
2. Duran CMG, Gunning AJ. A method for placing a total homologous aortic valve in the subcoronary position. *Lancet* 1962;2:488-489
3. Angell WW, Pupello DF, Bessone LN, Hiro SP. Universal method for insertion of unstented aortic autografts, homografts, and xenografts. *J Thorac Cardiovasc Surg* 1992;103:642-647; discussion 647-648
4. Duran CMG, Kumar N, Gometza B, Al Halees Z. Indications and limitations of aortic valve reconstruction. *Ann Thorac Surg* 1991;52:447-453; discussion 453-454
5. Duran CM, Gometza B, Kumar N, Gallo R, Martin-Duran R. Aortic valve replacement with freehand autologous pericardium. *J Thorac Cardiovasc Surg* 1995;110:511-516
6. David TE. Aortic root aneurysms: Remodeling or composite replacement? *Ann Thorac Surg* 1997;64:1564-1568
7. Yacoub MH, Gehle P, Chandrasekaran V, Birks EJ, Child A, Radley-Smith R. Late results of a valve-preserving operation in patients with aneurysms of the ascending aorta and root. *J Thorac Cardiovasc Surg* 1998;115:1080-1090
8. Leyh RG, Schmidtke C, Sievers HH, Yacoub MH. Opening and closing characteristics of the aortic valve after different types of valve-preserving surgery. *Circulation* 1999;100:2153-2160
9. Robicsek F, Leonardo da Vinci and the sinuses of Valsalva. *Ann Thorac Surg* 1991;52:328-335
10. Bellhouse BJ, Bellhouse FH. Mechanism of closure of the aortic valve. *Nature* 1968;217:86-87
11. Brewer RJ, Deck JD, Capati B, Nolan SP. The dynamic aortic root. Its role in aortic valve function. *J Thorac Cardiovasc Surg* 1976;72:413-417
12. Thubrikar M, Harry R, Nolan SP. Normal aortic valve function in dogs. *Am J Cardiol* 1977;40:563-568
13. Thubrikar M, Bosher LP, Nolan SP. The mechanism of opening of the aortic valve. *J Thorac Cardiovasc Surg* 1979;77:863-870
14. Vollebergh FE, Becker AE. Minor congenital variations of cusp size in tricuspid aortic valves. Possible link with isolated aortic stenosis. *Br Heart J* 1977;39:1006-1011
15. Choo SJ, McRae G, Olomon JP, et al. Aortic root geometry: Pattern of differences between leaflets and sinuses of Valsalva. *J Heart Valve Dis* 1999;8:407-415
16. van Renterghem R, van Steenhoven A, Arts T, Reneman R. Deformation of the dog aortic valve during the cardiac cycle. *Eur J Physiol* 1988;412:647-653
17. Dagum P, Green GR, Nistal FJ, et al. Deformational dynamics of the aortic root: Modes and physiologic determinants. *Circulation* 1999;100:II54-II62
18. Gorman JH, III, Gupta KB, Streicher JT, et al. Dynamic three-dimensional imaging of the mitral valve and left ventricle by rapid sonomicrometry array localization. *J Thorac Cardiovasc Surg* 1996;112:712-726
19. Hansen B, Menkis AH, Vesely I. Longitudinal and radial distensibility of the porcine aortic root (see comments). *Ann Thorac Surg* 1995;60:S384-S390
20. Pang DC, Choo SJ, Luo HH, et al. Significant increase of aortic root volume and commissural area occurs prior to aortic valve opening. *J Heart Valve Dis* 2000;9:9-15
21. Guyton AC. *Textbook of Medical Physiology*, 9th edn. Philadelphia: WB Saunders, 1996
22. Mountcastle VB. *Medical Physiology*, 13th edn. St. Louis: CV Mosby, 1974:892-893
23. Fung YC. *Biomechanics: motion, flow, stress, and growth*. New York: Springer-Verlag, 1990:358
24. Pappas T. *Heron's Theorem. The Joy of Mathematics*. San Carlos, CA: Wide World Publishing/Tetra, 1989:62
25. Fung YC. *Biomechanics: mechanical properties of living tissues*, 2nd edn. New York: Springer-Verlag, 1993:29-34
26. Popov EP. *Engineering Mechanics of Solids*. Upper Saddle River, NJ: Prentice-Hall, 1990:189
27. Sands MP, Rittenhouse EA, Mohri H, Merendino KA. An anatomical comparison of human, pig, calf, and sheep aortic valves. *Ann Thorac Surg* 1969;8:407-414
28. Kunzelman KS, Grande KJ, David TE, Cochran RP, Verrier ED. Aortic root and valve relationships. Impact on surgical repair. (Published erratum appears in *J Thorac Cardiovasc Surg* 1994

Jun;107:1402). J Thorac Cardiovasc Surg 1994;107:162-170  
 29. Sahasakul Y, Edwards WD, Naessens JM, Tajik AJ. Age-related changes in aortic and mitral valve thickness: Implications for two-dimensional echocardiography based on an autopsy study of 200 normal human hearts. Am J Cardiol

1988;62:424-430  
 30. Grande KJ, Cochran RP, Reinhall PG, Kunzelman KS. Stress variations in the human aortic root and valve: The role of anatomic asymmetry. Ann Biomed Eng 1998;26:534-545

Appendix I: Calculation of parameters.

Heron's formula

Given the lengths of the sides  $a$ ,  $b$ , and  $c$ , and the semi-perimeter,  $s$ , of a triangle:

$$s \equiv \frac{1}{2} (a + b + c)$$

Heron's formula gives the area  $\Delta$  of the triangle as:

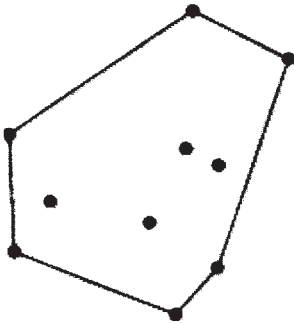
$$\Delta = \sqrt{s(s-a)(s-b)(s-c)}$$

Larangian strain

A unit strain defined as the ratio of (a) the change in length of a line segment to (b) its initial length.

$$S = \Delta l / l_0$$

Convex hull

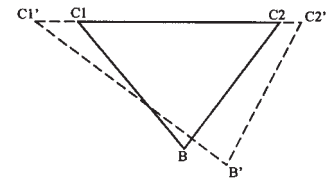


The convex hull of a set of points  $S$  in  $n$  dimensions is the intersection of all convex sets containing  $S$ . For  $N$  points  $p^1, \dots, p^N$ , the convex hull  $C$  is then given by the expression:

$$C \equiv \left\{ \sum_{j=1}^N \lambda_j p^j : \lambda_j \geq 0 \text{ for all } j \text{ and } \sum_{j=1}^N \lambda_j = 1 \right\}.$$

Shear angle

$$\text{Shear angle } \theta = \angle C_1BC_2 - \angle C_1'B'C_2'$$



(Clockwise)

Twist angle

Twist angle,  $d\theta = \delta / r$ , where  $r$  is the root radius and  $\delta$  is given by root height,  $dz$  multiplied by  $\tan$  (shear angle).

